The Design, Synthesis, and Evaluation of Organ-Specific Iron Chelators

Raymond J. Bergeron,* Jan Wiegand, James S. McManis, and Neelam Bharti

Department of Medicinal Chemistry, University of Florida, Gainesville, Florida 32610-0485

A series of iron chelators, three (*S*)-4,5-dihydro-2-(2-hydroxyphenyl)-4-methyl-4-thiazolecarboxylic acid (DADFT) and three (*S*)-4,5-dihydro-2-(2-hydroxyphenyl)-4-thiazolecarboxylic acid (DADMDFT) analogues are synthesized and assessed for their lipophilicity (log P_{app}), iron-clearing efficiency (ICE) in rodents and iron-loaded primates (*Cebus apella*), toxicity in rodents, and organ distribution in rodents. The results lead to a number of generalizations useful in chelator design strategies. In rodents, while log P_{app} is a good predictor of a chelator's ICE, chelator liver concentration is a better tool. In primates, log P_{app} is a good predictor of ICE, but only when comparing structurally very similar chelators. There is a profound difference in toxicity between the DADMDFT and DADFT series: DADMDFTs are less toxic. Within the DADFT family of ligands, the more lipophilic ligands are generally more toxic. Lipophilicity can have a profound effect on ligand organ distribution, and ligands can thus be targeted to organs compromised in iron overload disease, for example, the heart.

Introduction

Iron is essential to redox processes in all prokaryotes and eukaryotes. Although this element comprises 5% of the earth's crust, living systems have great difficulty in accessing and managing this vital micronutrient. The low solubility of Fe(III) hydroxide ($K_{sp} = 1 \times 10^{-39}$),[1] the predominant form of the metal in the biosphere, has led to the development of sophisticated iron storage and transport systems in nature. Microorganisms utilize low molecular weight, virtually ferric iron-specific ligands, siderophores;[2] higher eukaryotes tend to employ proteins to transport and store iron (e.g., transferrin and ferritin, respectively).[3−5]

Higher life forms, for example, humans, have developed a highly efficient iron management system in which we absorb and excrete only about 1 mg of the metal daily; there is no mechanism for the excretion of excess iron.[6] Whether a systemic or a focal problem, the toxicity associated with excess iron derives from its interaction with reactive oxygen species, for instance, endogenous hydrogen peroxide (H_2O_2).[7−10] In the presence of Fe(II), H_2O_2 is reduced to the hydroxyl radical (HO•) and HO−, a process known as the Fenton reaction. The hydroxyl radical reacts very quickly with a variety of cellular constituents and can initiate free radicals and radical-mediated chain processes that damage DNA and membranes, as well as produce carcinogens.[8,11,12] The Fe(III) liberated in the peroxide reduction can be converted back to Fe(II) via a variety of biological reductants (e.g., ascorbate), a problematic cycle.

Whether derived from transfused red blood cells[13−15] or from increased absorption of dietary iron,[16,17] without effective treatment, body iron progressively increases with deposition in the liver, heart, pancreas, and elsewhere. Iron accumulation eventually produces liver disease that may progress to cirrhosis,[18−20] diabetes related both to iron-induced decreases in pancreatic β-cell secretion and to increases in hepatic insulin resistance,[21,22] and heart disease, still the leading cause of death in thalassemia major and related forms of transfusional iron overload.[6,23,24] The precise pathways of iron deposition and its regulation are 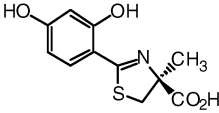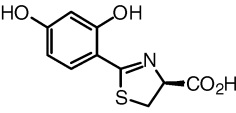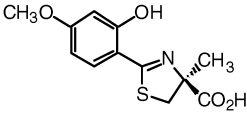incompletely unders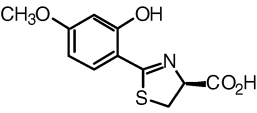tood, but the available evidence suggests that these differ in the liver, physiologically a major systemic iron depot, and in the pancreas and heart, which normally do not serve as iron storage sites. Nontransferrin-bound plasma iron (NTBI), a heterogeneous pool of iron in the circulation that is not bound to the physiological iron transporter, transferrin, seems to be a principal source of the abnormal tissue distribution of iron that develops with chronic iron overload. NTBI is rapidly taken up by hepatocytes in the liver, the major iron storage organ, perhaps through the divalent metal transporter 1[25] and other pathways that remain poorly characterized. NTBI also seems to gain entry into cardiomyocytes, pancreatic β-cells, and anterior pituitary cells specifically via L-type voltage-dependent Ca^{2+} channels not found in hepatoc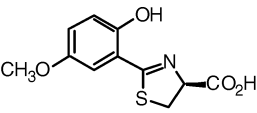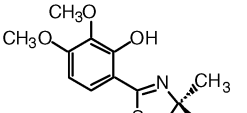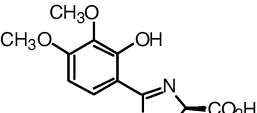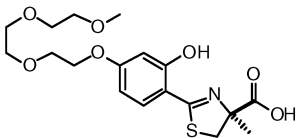ytes or Kupffer cells.[26] These differences in modes of iron uptake also may underlie clinical observations of differences in the course and pace of iron deposition and damage to the liver, pancreas, and heart in patients with all forms of iron overload.[6]
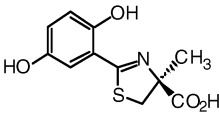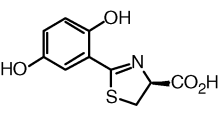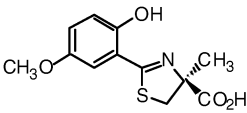
In the majority of patients with thalassemia major or other transfusion-dependent refractory anemias, the severity of the anemia precludes phlebotomy therapy as a means of removing toxic accumulations of iron. Treatment with a chelating agent capable of sequestering iron and permitting its excretion from

---

a Abbreviations: DADFT, desazadesferrithiocin [(*S*)-4,5-dihydro-2-(2-hydroxyphenyl)-4-methyl-4-thiazolecarboxylic acid]; DADMDFT, desaza-desmethyldesferrithiocin [(*S*)-4,5-dihydro-2-(2-hydroxyphenyl)-4-thiazole-carboxylic acid]; ICE, iron-clearing efficiency; log P_{app}, octanol−water partition coefficient (lipophilicity); DFO, desferrioxamine B mesylate; DFT, desferrithiocin [(*S*)-4,5-dihydro-2-(3-hydroxy-2-pyridinyl)-4-methyl-4-thia-zolecarboxylic acid]; NTBI, nontransferrin-bound iron; (*S*)-4′-(HO)-DADFT, **1**, (*S*)-2-(2,4-dihydroxyphenyl)-4,5-dihydro-4-methyl-4-thiazolecarboxylic acid; (*S*)-4′-(CH₃O)-DADFT, **2**, (*S*)-4,5-dihydro-2-(2-hydroxy-4-methoxy-phenyl)-4-methyl-4-thiazolecarboxylic acid; (*S*)-5′-(HO)-DADFT, **3**, (*S*)-2-(2,5-dihydroxyphenyl)-4,5-dihydro-4-methyl-4-thiazolecarboxylic acid; (*S*)-5′-(CH₃O)-DADFT, **4**, (*S*)-4,5-dihydro-2-(2-hydroxy-5-methoxyphenyl)-4-methyl-4-thiazolecarboxylic acid; (*S*)-3′,4′-(CH₃O)₂-DADFT, **5**, (*S*)-4,5-dihydro-2-(3,4-dimethoxy-2-hydroxyphenyl)-4-methyl-4-thiazolecarboxyl-ic acid; (*S*)-4′-(HO)-DADFT-PE, **6**, (*S*)-4,5-dihydro-2-[2-hydroxy-4-(3,6,9-trioxadecyloxy)phenyl]-4-methyl-4-thiazolecarboxylic acid; (*S*)-4′-(HO)-DADMDFT, **7**, (*S*)-2-(2,4-dihydroxyphenyl)-4,5-dihydro-4-thiazolecarboxylic acid; (*S*)-4′-(CH₃O)-DADMDFT, **8**, (*S*)-4,5-dihydro-2-(2-hydroxy-4-meth-oxyphenyl)-4-thiazolecarboxylic acid; (*S*)-5′-(HO)-DADMDFT, **9**, (*S*)-2-(2,5-dihydroxyphenyl)-4,5-dihydro-4-thiazolecarboxylic acid; (*S*)-5′-(CH₃O)-DADMDFT, **10**, (*S*)-4,5-dihydro-2-(2-hydroxy-5-methoxyphenyl)-4-thiazole-carboxylic acid; (*S*)-3′,4′-(CH₃O)₂-DADMDFT, **11**, (*S*)-4,5-dihydro-2-(3,4-dimethoxy-2-hydroxyphenyl)-4-thiazolecarboxylic acid.

* To whom correspondence should be addressed. Phone: (352) 846-1956. Fax: (352) 392-8406. E-mail: rayb@ufl.edu.

Table 1. Iron-Clearing Activity of Desferrithiocin Analogues When Administered Orally to Rodents and the Partition Coefficients of the Compounds

Desaza Series			Desazadesmethyl Series		
Desferrithiocin Analogue	Iron Clearing Efficiency (%)[a]	$\log P_{app}$[b]	Desferrithiocin Analogue	Iron Clearing Efficiency (%)[a]	$\log P_{app}$[b]
(S)-4'-(HO)-DADFT, **1**	1.1 ± 0.8[c] [100/0]	−1.05	(S)-4'-(HO)-DADMDFT, **7**	2.9 ± 2.8[d] [100/0]	−1.33
(S)-4'-(CH₃O)-DADFT, **2**	6.6 ± 2.8[c] [98/2]	−0.70	(S)-4'-(CH₃O)-DADMDFT, **8**	11.6 ± 5.1 [99/1]	−0.89
(S)-5'-(HO)-DADFT, **3**	1.0 ± 0.9 [99/1]	−1.14	(S)-5'-(HO)-DADMDFT, **9**	<0.05	−1.52
(S)-5'-(CH₃O)-DADFT, **4**	6.3 ± 1.2 [95/5]	−0.61	(S)-5'-(CH₃O)-DADMDFT, **10**	8.9 ± 3.8 [97/3]	−0.81
(S)-3',4'-(CH₃O)₂-DADFT, **5**	16.6 ± 8.6[e] [99/1]	−0.95	(S)-3',4'-(CH₃O)₂-DADMDFT, **11**	11.9 ± 1.0 [97/3]	−1.28
(S)-4'-(HO)-DADFT-PE, **6**	5.5 ± 1.9[c] [90/10]	−1.10			

[a] In the rodents [$n = 3$ (**9**), 4 (**2**, **3**, **4**, **7**, **8**, **11**), 5 (**5**, **6**, **10**), or 8 (**1**)], the dose was 150 μmol/kg for **9** and 300 μmol/kg for **1–8**, **10**, and **11**. The compounds were solubilized in either distilled water (**6**) or 40% Cremophor (**7** and **9**) or were given as their monosodium salts, prepared by the addition of 1 equiv of NaOH to a suspension of the free acid in distilled water (**1–5**, **8**, **10**, and **11**). The efficiency of each compound was calculated by subtracting the iron excretion of control animals from the iron excretion of the treated animals. This number was then divided by the theoretical output; the result is expressed as a percent. The relative percentages of the iron excreted in the bile and urine are in brackets. [b] Data are expressed as the log of the fraction in the octanol layer (log P_{app}); measurements were done in TRIS buffer, pH 7.4, using a "shake flask" direct method. The values obtained for compounds **1**, **2**, **7**, and **8** are from ref 38; the value for **6** is from ref 39. [c] Data are from ref 39. [d] Data are from ref 52. [e] ICE is based on a 48 h sample collection.

the body is then the only therapeutic approach available. The iron-chelating agents now in use or under clinical evaluation are desferrioxamine B mesylate (DFO[a]), 1,2-dimethyl-3-hydroxy-pyridin-4-one (deferiprone, L1), 4-[3,5-bis(2-hydroxyphenyl)-1,2,4-triazol-1-yl]benzoic acid (deferasirox, ICL670A), and our own desferrithiocin (DFT) analogue, (S)-2-(2,4-dihydroxyphenyl)-4,5-dihydro-4-methyl-4-thiazolecarboxylic acid [deferitrin, (S)-4′-(HO)-DADFT, **1**, Table 1]. Each of these agents chelates iron derived predominantly from systemic storage sites, from iron released by macrophages after catabolism of senescent red blood cells, from iron in hepatic pools, or from both.[27]

In patients, treatment with DFO can sometimes improve cardiomyopathy within days, before the total iron burden could have changed appreciably.[28] Nonetheless, the amounts of iron removed from the heart are small; daily 24-hour infusions of

DFO are then required for periods of years to reverse iron-induced heart disease completely.[28] The efficacy of deferiprone in patients with heart disease remains uncertain, and deferasirox likely does not enter the heart in appreciable amounts. In any event, almost daily administration of near maximal tolerated doses of the first three agents is required to keep pace with rates of transfusional iron loading in patients with thalassemia major and other refractory anemias[29] and thereby minimize the amounts of circulating NTBI. Consequently, there is a pressing need for the continued development of new iron-chelating agents that are more efficient and that can selectively remove iron from organs and tissues especially vulnerable to iron-induced toxicity. Ligands that are more efficient would be able to more rapidly reduce dangerous body iron burdens to safer levels and forestall the development or progression of complications. Iron-chelating

agents that could selectively enter cardiac, pancreatic, or hepatic cells could help immediately reduce toxic iron pools and provide prompt protection against the progression of injury. This is especially true with respect to heart disease, still the cause of death in 70% or more of patients with thalassemia major;[13,23,24] the development of such agents could be life-saving.

Results and Discussion

Design Concept. DFT is a tridentate siderophore[30] that forms a stable 2:1 complex with Fe(III)[31,32] and clears the metal well when the ligand is given orally (po) in both the bile duct-cannulated rodent model (iron-clearing efficiency, ICE, 5.5%)[33] and in the iron-overloaded *Cebus apella* primate (ICE, 16%).[34,35] However, DFT is severely nephrotoxic.[35] Nevertheless, its oral activity spurred a structure−activity study focused on identifying an orally active and safe DFT analogue.

The structure−activity study first entailed simplifying the platform. For example, removal of the pyridine nitrogen of DFT led to (*S*)-4,5-dihydro-2-(2-hydroxyphenyl)-4-methyl-4-thiazolecarboxylic acid [(*S*)-DADFT], still a very effective iron chelator, although the ligand now presented with gastrointestinal toxicity rather than nephrotoxicity.[36] It was next demonstrated that hydroxylation of this and related desaza ligands was compatible with iron clearance in the primate model and provided much less toxic chelators.[36−38] As previously mentioned, one of these ligands, (*S*)-4′-(HO)-DADFT (**1**; Table 1), is now in clinical trials for treatment of iron overload. However, animal studies indicate that the dose-limiting toxicity of this chelator will still likely be nephrotoxicity.[37] Although the origin of the nephro-toxicity is unclear, the target seems to be centered largely in the proximal tubules. Recently, we were able to show that conversion of **1** to the corresponding polyether (*S*)-4,5-dihydro-2-[2-hydroxy-4-(3,6,9-trioxadecyloxy)phenyl]-4-methyl-4-thia-zolecarboxylic acid [(*S*)-4′-(HO)-DADFT-PE, **6**, Table 1] ameliorated much of the problem simply by reducing the level of drug in the kidney. The polyether had a substantially better ICE in both the rat and the primate than the parent drug (**1**) and greatly reduced nephrotoxicity.[39]

In the course of our structure−activity studies focused on developing an acceptable toxicity profile, the significance of lipophilicity, log P_{app}, in chelator design became apparent. The ligands' log P_{app} often correlated with iron-clearing efficiency (Tables 1 and 2), toxicity (Table 3), and organ distribution (Figures 1 and 2). Within a series, or family, of ligands, the more lipophilic compounds generally have better iron-clearing efficiency, that is, the larger the log P_{app} value of the compound, the greater the iron-clearing efficiency. As will be seen below, the impact of lipophilicity on chelator toxicity can be very significant, although it is very much dependent on the family of ligands. Finally, data consistently shows lipophilicity to have a profound effect on organ distribution of the chelator (Figures 1 and 2); the more lipophilic ligands typically achieve higher concentrations of drug and/or remain longer in organs. For example, (*S*)-4,5-dihydro-2-(2-hydroxy-4-methoxyphenyl)-4-methyl-4-thiazolecarboxylic acid [(*S*)-4′-(CH₃O)-DADFT, **2**] achieves between two and three times the concentration of chelator in the heart and pancreas than does administration of the parent (*S*)-4′-(HO)-DADFT (**1**; Figure 1). If it were not for the poor toxicity profile of **2**,[39] it might be of great value for removing cardiac iron.

The current study further defines the role of ligand lipo-philicity in iron-clearing efficiency, toxicity, and organ distribu-tion with the intent of identifying ligands that achieve high and prolonged cardiac levels and present with an acceptable toxicity

profile. Again, iron-mediated cardiac damage is the main cause of mortality in iron overload disease.

Two ligand families are assessed, the (*S*)-4,5-dihydro-2-(2-hydroxyphenyl)-4-methyl-4-thiazolecarboxylic acids (DADFTs, **1**−**6**) and the (*S*)-4,5-dihydro-2-(2-hydroxyphenyl)-4-thiazole-carboxylic acids (DADMDFTs, **7**−**11**; Table 1). The new ligands in the DADFT series include (*S*)-2-(2,5-dihydroxyphe-nyl)-4,5-dihydro-4-methyl-4-thiazolecarboxylic acid [(*S*)-5′-(HO)-DADFT, **3**], (*S*)-4,5-dihydro-2-(2-hydroxy-5-methoxyphe-nyl)-4-methyl-4-thiazolecarboxylic acid [(*S*)-5′-(CH₃O)-DADFT, **4**], and (*S*)-4,5-dihydro-2-(3,4-dimethoxy-2-hydroxyphenyl)-4-methyl-4-thiazolecarboxylic acid [(*S*)-3′,4′-(CH₃O)₂-DADFT, **5**]. The new ligands in the DADMDFT series include (*S*)-2-(2,5-dihydroxyphenyl)-4,5-dihydro-4-thiazolecarboxylic acid [(*S*)-5′-(HO)-DADMDFT, **9**], (*S*)-4,5-dihydro-2-(2-hydroxy-5-meth-oxyphenyl)-4-thiazolecarboxylic acid [(*S*)-5′-(CH₃O)-DADMDFT, **10**], and (*S*)-4-5-dihydro-2-(3,4-dimethoxy-2-hydroxyphenyl)-4-thiazolecarboxylic acid [(*S*)-3′,4′-(CH₃O)₂-DADMDFT, **11**]. The DADMDFT chelators previously studied in this laboratory consist of (*S*)-2-(2,4-dihydroxyphenyl)-4,5-dihydro-4-thiazole-carboxylic acid [(*S*)-4′-(HO)-DADMDFT, **7**][36] and (*S*)-4,5-dihydro-2-(2-hydroxy-4-methoxyphenyl)-4-thiazolecarboxylic acid [(*S*)-4′-(CH₃O)-DADMDFT, **8**].[38]

Synthetic Methods. Cyclocondensation of the appropriately substituted 2-hydroxybenzonitrile (**12**−**14**) with (*S*)-α-methyl cysteine (**15**) in aqueous CH₃OH buffered at pH 6 furnished DADFTs **3**−**5**; use of (*S*)-cysteine (**16**) instead gave the corresponding DADMDFTs **9**−**11** (Scheme 1). Treatment of 2,5-dimethoxybenzonitrile (**17**) with boron tribromide in CH₂-Cl₂ produced 2,5-dihydroxybenzonitrile (**12**) in 80% yield (Scheme 2). Upon heating nitrile **12** with amino acid **15** or **16** near neutrality, (*S*)-5′-(HO)-DADFT (**3**; 97% yield) or (*S*)-5′-(HO)-DADMDFT (**9**; 75% yield), respectively, was obtained. 2-Hydroxy-5-methoxybenzonitrile (**13**),[40] when heated with amino acid **15**, led to (*S*)-5′-(CH₃O)-DADFT (**4**) in 99% yield. Condensation of nitrile **13** with D-cysteine (**16**) gave (*S*)-5′-(CH₃O)-DADMDFT (**10**) in 77% yield (Scheme 1). 3,4-Dimethoxy-2-hydroxybenzaldehyde (**18**)[41,42] was converted to its oxime **19** in 84% yield using hydroxylamine hydrochloride and NaOAc in CH₃OH. Dehydration of **19** with refluxing acetic anhydride and saponification of the aryl acetate intermediate gave 3,4-dimethoxy-2-hydroxybenzonitrile (**14**) in 82% yield (Scheme 3). Cyclization of amino acid **15** or **16** with aryl cyanide **14** at pH 6 produced (*S*)-3′,4′-(CH₃O)₂-DADFT (**5**; 60% yield) or (*S*)-3′,4′-(CH₃O)₂-DADMDFT (**11**; 76% yield), respec-tively (Scheme 1).

Chelator-Induced Iron Clearance in Non-Iron-Overloaded Rodents. Iron-clearing efficiencies of the compounds in rats are shown (Table 1), along with the relative fractions of the iron excreted in the bile and in the urine. A single 150 μmol/kg (**9**) or 300 μmol/kg (**1**−**8**, **10**, **11**) dose of drug was administered orally by gavage to male Sprague−Dawley rats. The data will be discussed within the sets of ligands, that is, DADFT chelators [**1**, **2**], [**3**, **4**], [**5**], [**6**] and DADMDFT ligands [**7**, **8**], [**9**, **10**], [**11**]. Recall that iron clearing efficiency (ICE) is defined as (net iron excretion)/(total iron-binding capacity of the chelator), expressed as a percent. The previous studies with ligands [**1**, **2**] and [**7**, **8**] clearly indicated that the more lipophilic chelators had greater ICE values.[43] In the current study with [**3**, **4**] and [**9**, **10**], again the more lipophilic ligand was the more efficient (**4** > **3**, $p < 0.001$ and **10** > **9**, $p < 0.003$). While the polyether (**6**) follows the expected trend, the dimethoxy systems **5** and **11** were not well behaved within the DADFT and DADMDFT families; their ICEs were higher than anticipated. However, this

Table 2. Iron-Clearing Activity of Desferrithiocin Analogues When Administered Orally to *Cebus apella* Primates and the Partition Coefficients of the Compounds
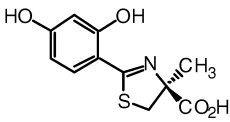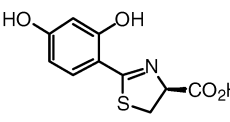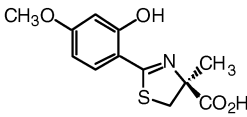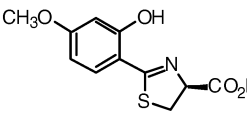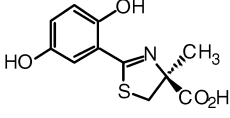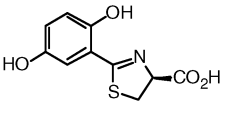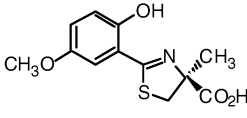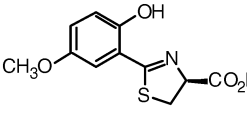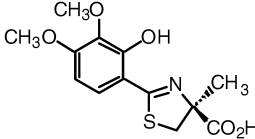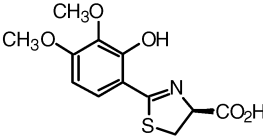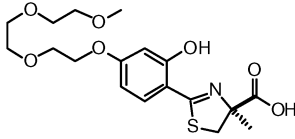
Desaza Series			Desazadesmethyl Series		
Desferrithiocin Analogue	Iron Clearing Efficiency (%)[a]	log P_{app}[b]	Desferrithiocin Analogue	Iron Clearing Efficiency (%)[a]	log P_{app}[b]
(*S*)-4'-(HO)-DADFT, **1**	16.8 ± 7.2[c] [88/12]	−1.05	(*S*)-4'-(HO)-DADMDFT, **7**	4.2 ± 1.4[d] [70/30]	−1.33
(*S*)-4'-(CH₃O)-DADFT, **2**	24.4 ± 10.8[e] [91/9]	−0.70	(*S*)-4'-(CH₃O)-DADMDFT, **8**	16.2 ± 3.2[e] [81/19]	−0.89
(*S*)-5'-(HO)-DADFT, **3**	12.6 ± 3.0 [88/12]	−1.14	(*S*)-5'-(HO)-DADMDFT, **9**	1.8 ± 0.8 [97/3]	−1.52
(*S*)-5'-(CH₃O)-DADFT, **4**	18.9 ± 2.3 [94/6]	−0.61	(*S*)-5'-(CH₃O)-DADMDFT, **10**	12.0 ± 6.6 [97/3]	−0.81
(*S*)-3',4'-(CH₃O)₂-DADFT, **5**	Not Tested[f]	−0.95	(*S*)-3',4'-(CH₃O)₂-DADMDFT, **11**	12.4 ± 6.3 [94/6]	−1.28
(*S*)-4'-(HO)-DADFT-PE, **6**	25.4 ± 7.4[g] [96/4]	-1.10			

[a] In the monkeys [*n* = 4 (**3**, **4**, **6**−**9**), 3 (**10**), 6 (**1**, **11**), or 7 (**2**)], the dose was 150 μmol/kg. The compounds were solubilized in either distilled water (**6**) or 40% Cremophor (**2**, **7**, **8**) or were given as their monosodium salts, prepared by the addition of 1 equiv of NaOH to a suspension of the free acid in distilled water (**1**, **3**, **4**, **9**−**11**). The efficiency of each compound was calculated by averaging the iron output for 4 days before the administration of the drug, subtracting these numbers from the 2-day iron clearance after the administration of the drug, and then dividing by the theoretical output; the result is expressed as a percent. The relative percentages of the iron excreted in the stool and urine are in brackets. [b] Data are expressed as the log of the fraction in the octanol layer (log P_{app}); measurements were done in TRIS buffer, pH 7.4, using a "shake flask" direct method. The values obtained for compounds **1**, **2**, **7**, and **8** are from ref 38; the value for **6** is from ref 39. [c] Data are from ref 37. [d] Data are from ref 36. [e] Data are from ref 38. [f] Not tested in the primates due to acute toxicity in mice (data not shown). [g] Data are from ref 39.

apparent discrepancy may be explained by liver chelator concentrations (Figures 1 and 2). This is consistent with the idea that for the lipophilicity/ICE relationship to hold, the extent of aromatic ring functionalization must remain similar. Additionally, there was no clear trend between log P_{app} and modes of iron excretion, for example, urinary versus biliary. Finally, it is noteworthy that moving 4′-hydroxyl of **7** to the 5′-position providing ligand **9** had a significant effect on both decreasing lipophilicity and reducing the ICE, 3% to <0.05%, *p* < 0.05. This was not the case with ligands **1** and **3** of the DADFT series (Table 1). Although the log P_{app} of these ligands changed by a similar magnitude as **7** to **9**, there was little effect on ICE (*p* > 0.05).

Relationship between Rodent ICE and Liver Chelator Concentration. In rodents, while the ICE of the monosubstituted DADFT and DADMDFT analogues correlated well with the lipophilicity of the ligands, this was not the case with the disubstituted chelators **5** and **11**; their ICE was much higher than expected. However, an examination of the liver concentration of the DADFT ligands 0.5 h postdrug versus the ICE of the drugs (Figure 3) reveals that as the liver tissue concentration of the chelators increases, the ICE also increases (r^2 = 0.965). This scenario was also seen with the DADMDFT analogues (r^2 = 0.953, data not shown). Note that although the chelators were given subcutaneously (sc) in the tissue distribution studies and po in the ICE experiments, we have previously demon-

Table 3. Partition Coefficients and Rodent Tolerability of DADFT and DADMDFT Analogues

Desaza Series			Desazadesmethyl Series		
Desferrithiocin Analogue	Log P_{app}	Tolerability[a]	Desferrithiocin Analogue	Log P_{app}	Tolerability[a]
(S)-4'-(HO)-DADFT, **1**	−1.05	All survived.[b]	(S)-4'-(HO)-DADMDFT, **7**	−1.33	All survived.[b]
(S)-4'-(CH₃O)-DADFT, **2**	−0.70	All dead by day 6.[c]	(S)-4'-(CH₃O)-DADMDFT, **8**	−0.89	All survived.[d]
(S)-5'-(HO)-DADFT, **3**	−1.14	All survived.	(S)-5'-(HO)-DADMDFT, **9**	−1.52	All survived.
(S)-5'-(CH₃O)-DADFT, **4**	−0.61	All dead by day 7.	(S)-5'-(CH₃O)-DADMDFT, **10**	−0.81	All survived.
(S)-3',4'-(CH₃O)₂-DADFT, **5**	−0.95	All dead by day 10.	(S)-3',4'-(CH₃O)₂-DADMDFT, **11**	−1.28	All survived.
(S)-4'-(HO)-DADFT-PE, **6**	−1.10	All survived.[c]			

[a] The compounds were given to the rats orally by gavage at a dose of 384 μmol/kg/d for a maximum of 10 days. [b] Toxicity data are from ref 37. [c] Toxicity data are from ref 39. [d] Toxicity data are from ref 43.

strated, for example, (S)-4'-(CH₃O)-DADFT (**2**), that the ligands have a very high oral bioavailability and that there was little difference in the tissue distribution of po versus sc administered chelators.[43] Thus, liver chelator concentration may be a more predictive tool of ICE in rodents than log P_{app}.

Chelator-Induced Iron Clearance in Iron-Overloaded Primates. The drugs were given po to the monkeys at a dose of 150 μmol/kg (Table 2). In every instance, the ligands' ICE values were higher in iron-overloaded primates than in the non-iron-loaded rodents (Table 1). The difference in ICE values between species is not surprising in view of the larger, accessible iron pool in the iron-overloaded primates. Again, looking at the sets of DADFT chelators [**1, 2**], [**3, 4**], [**6**] and DADMDFT ligands [**7, 8**], [**9, 10**], [**11**] (Table 2), the trend is similar to the rodents regarding lipophilicity, with some leveling effect probably due to more available iron for chelation. With the sets [**1, 2**] and [**7, 8**], the more lipophilic molecules had the better ICE values.[43] Again, the more lipophilic compounds are more active (**3** vs **4**, $p < 0.01$) and (**9** vs **10**, $p = 0.05$). However, with the polyether (**6**) there is a rather surprising jump in

efficiency (Table 2). This polyether behaves more like its (S)-4'-(CH₃O)-DADFT analogue (**2**) than would be predicted on the basis of lipophilicity. While we were unwilling to evaluate the iron clearance properties of dimethoxy DADFT analogue **5** in primates because of its unexpected acute toxicity in mice (not described), the dimethoxy DADMDFT analogue **11** was more efficient at iron clearance than would be predicted from its log P_{app} value.

Again, there was no clear relationship between modes of excretion, biliary versus urinary, and log P_{app}. Once again, it is noteworthy that a simple shift of the 4'-(HO) to the 5' position decreased the ICE from 4 to 2% for the [**7, 9**] set ($p < 0.02$) and from 17 to 13% for the [**1, 3**] set, although the decrease was not significant (Table 2).

Relationship between Toxicity and Lipophilicity. The toxicity trials were carried out in male Sprague−Dawley rats. The animals were given the chelators orally by gavage at a dose of 384 μmol/kg/d for a maximum of 10 days. The dose, which is equivalent to 100 mg/kg of the DFT monosodium salt, was chosen to compare toxicity with previous data.[37,39,43] There are
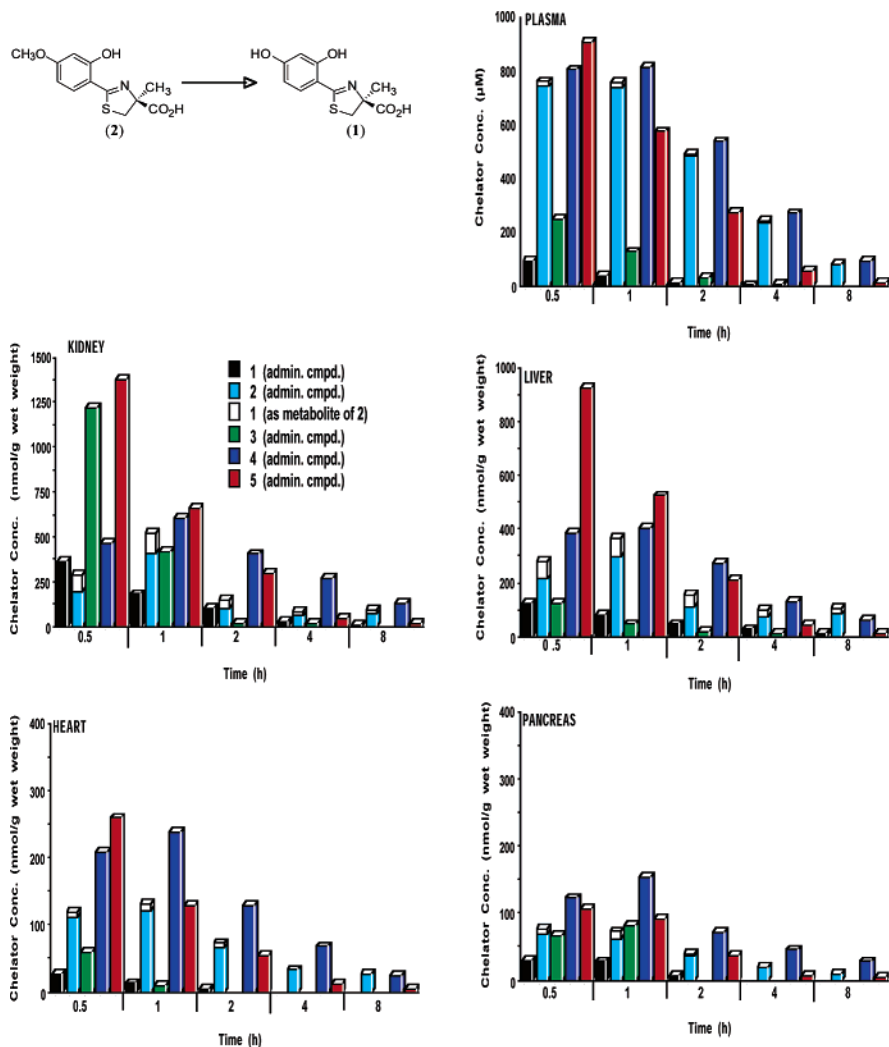
Figure 1. Tissue distribution in plasma, kidney, liver, heart, and pancreas of rats treated with DADFT analogues **1**−**5** given sc at a dose of 300 μmol/kg. The concentrations (y-axis) are reported as μM (plasma) or as nmol compound per g wet weight of tissue. For all time points, $n = 3$. The demethylation in the liver of **2** → **1** is also shown.

two obvious relationships bearing on the toxicity profiles of the DFT analogues evaluated (Table 3): (1) the DADMDFT ligands (**7**−**11**) are generally less toxic than the corresponding DADFT series (**1**−**5**) and (2) while the DADMDFT ligand toxicity profiles are independent of partition properties, this is not the case with the DADFT analogues. Within the DADFT sets [**1** vs **2**] and [**3** vs **4**], the less lipophilic ligand was also the less toxic. When rodents were treated with DADFT chelators with log P_{app} values greater than −1.05 at 384 μmol/kg/d, all of the animals were dead before the end of the planned 10-day dosing regimen. This same relationship also held up with dimethoxy analogue (**5**) and the polyether (**6**). The polyether (log P_{app} = −1.10) was profoundly less toxic than **5** (Table 3). In each instance of mortality (**2**, **4**, **5**), the rats presented with nephrotoxicity, which was acute, diffuse, and severe and characterized by proximal tubular epithelial necrosis and sloughing.

Chelator Tissue Distribution in Rodents. The tissue distribution description will focus first on the DADFT ligands [**1**, **2**], [**3**, **4**], [**5**] (Figure 1) and next on the DADMDFT analogues [**7**, **8**], [**9**, **10**], [**11**] (Figure 2). In each instance, we will consider plasma, kidney, liver, heart, and pancreas. In these studies, the rats were given a single 300 μmol/kg dose of the drug sc. Subcutaneous administration was chosen to minimize possible, but unlikely, complications surrounding differences in oral absorption.

Desazadesferrithiocin Analogues. In the case of the DADFT analogues in the plasma (Figure 1), the more lipophilic systems achieve much higher concentrations and maintain them for a longer period of time. The parent drug (S)-4′-(HO)-DADFT (**1**) reaches a level of 92 μM at 0.5 h and drops to 13 μM at 2 h. The methoxy analogue **2** (plus its metabolite **1**) reaches nearly eight times the level of the parent **1** ($p < 0.002$) at 0.5 h. Even at 8 h the concentration of the methoxy **2** is still as high as the initial level of the parent **1**. A similar scenario is true for (S)-5′-(HO)-DADFT (**3**) and its methylated analogue (S)-5′-(CH$_3$O)-DADFT (**4**). At 0.5 h, the more lipophilic **4**, at a concentration of 803 μM, reaches more than three times the concentration of **3** ($p < 0.001$). It is noteworthy that the 5′-substituted ligands achieve higher plasma levels than the 4′-substituted ligands (Figure 1). The (S)-3′,4′-(CH$_3$O)$_2$-DADFT analogue (**5**) achieves the highest initial plasma concentration of all of the DADFT analogues (907 μM, $p < 0.001$ for **1** and **3** and $p < 0.05$ for **2** and **4**), although it is essentially gone by 8 h.

In the kidney, the situation is a little different (Figure 1). The parent **1** and its methoxy analogue **2** achieve similar initial concentrations at 0.5 h (361 vs 282 nmol/g wet weight, respectively, $p > 0.05$). However, at 1 h postdrug, **2** (plus its metabolite **1**) is nearly three times the concentration of the parent **1** (518 vs 179 nmol/g wet weight, respectively, $p < 0.002$), then decreasing, although always at higher levels than the parent
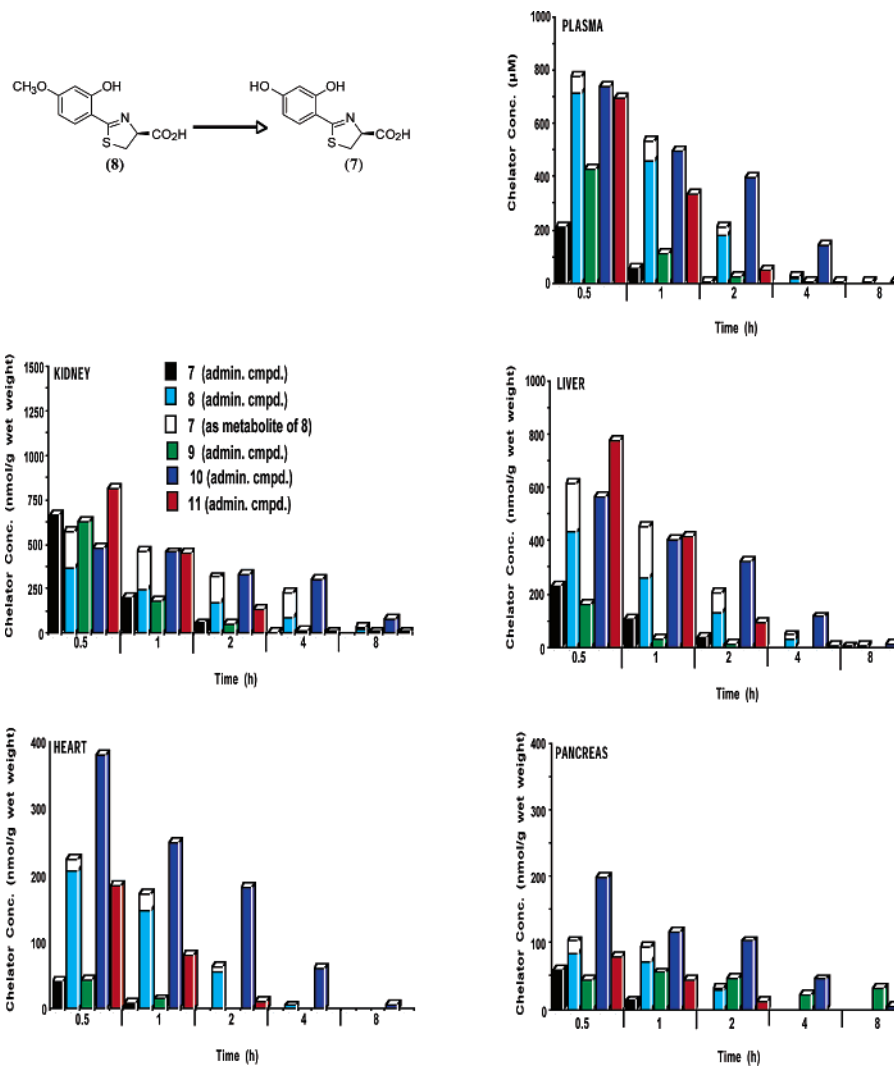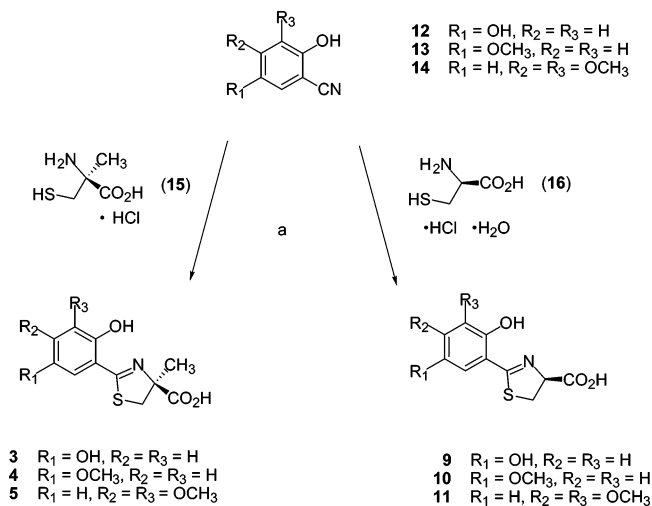
Figure 2. Tissue distribution in plasma, kidney, liver, heart, and pancreas of rats treated with DADMDFT analogues **7**−**11** given sc at a dose of 300 μmol/kg. The concentrations (*y*-axis) are reported as μM (plasma) or as nmol compound per g wet weight of tissue. For all time points, $n = 3$. The demethylation in the liver of **8** → **7** is also shown.

Scheme 1. Synthesis of DADFTs **3**−**5** and DADMDFTs **9**−**11**[a]

3 R₁ = OH, R₂ = R₃ = H
4 R₁ = OCH₃, R₂ = R₃ = H
5 R₁ = H, R₂ = R₃ = OCH₃

9 R₁ = OH, R₂ = R₃ = H
10 R₁ = OCH₃, R₂ = R₃ = H
11 R₁ = H, R₂ = R₃ = OCH₃

12 R₁ = OH, R₂ = R₃ = H
13 R₁ = OCH₃, R₂ = R₃ = H
14 R₁ = H, R₂ = R₃ = OCH₃

[a] Reagents: (a) CH₃OH (aq), pH 6, heat, ≥1 d.

Scheme 2. Preparation of 2,5-Dihydroxybenzonitrile (**12**)[a]
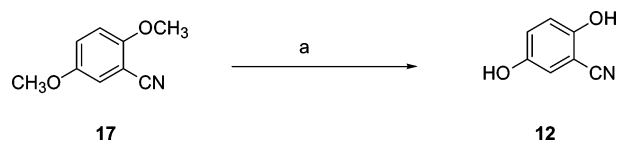
[a] Reagents: (a) BBr₃, CH₂Cl₂ (80%).

analogue **4** at 0.5 h ($p < 0.002$), although the parent drug **3** levels drop very quickly, by 98% at 2 h. Finally, the (*S*)-3′,4′-dimethoxy chelator (**5**) achieves the highest initial renal tissue concentration of all the DADFT analogues (1375 nmol/g wet weight, $p < 0.001$ for **1**, **2**, and **4**), although it drops quickly, almost mirroring the plasma levels.

The liver tissue concentrations for ligands **1**−**4** (Figure 1) display a trend similar to plasma at each time point; the more lipophilic methoxylated ligands achieve and maintain greater levels than the hydroxylated parent drugs. The parent **1** reaches 124 nmol/g wet weight at 0.5 h, while its methoxy analogue **2** (plus its metabolite **1**) rises to 275 nmol/g wet weight ($p < 0.05$). The 5′-(HO) analogue **3** at 0.5 h is very similar to **1**, while its 5′-(CH₃O) analogue **4** achieves 382 nmol/g wet weight, $p < 0.001$ versus **3** (Figure 1). Again, the (*S*)-3′,4′-dimethoxy

1. A similar scenario holds for 5′-substituted ligands (Figure 1). The 5′-hydroxy parent ligand **3** (1216 nmol/g wet weight) achieves over twice the concentration of the 5′-methoxy

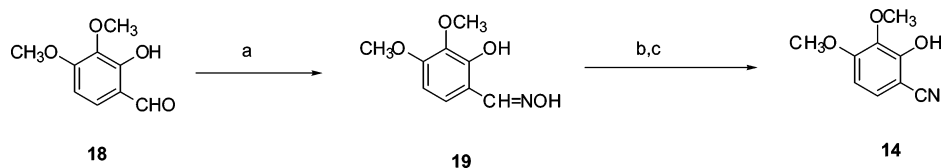**Scheme 3.** Preparation of 3,4-Dimethoxy-2-hydroxybenzonitrile (**14**)[a]

[a] Reagents: (a) $H_2NOH \cdot HCl$, NaOAc, CH_3OH (84%); (b) Ac_2O, reflux; (c) NaOH, CH_3OH (aq, 82%).
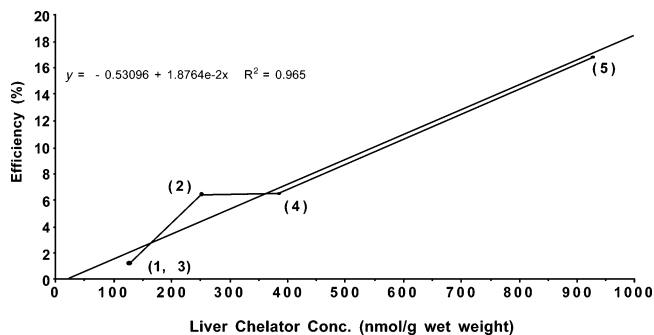

Figure 3. Iron-clearing efficiency of DADFT analogues **1**−**5** plotted vs the liver chelator concentration. The rats were given a single 300 $\mu mol/kg$ dose of the compounds po for the ICE determinations and sc for the tissue distribution studies.

analogue (**5**) reaches the highest liver concentration (924 nmol/g wet weight, $p < 0.001$ vs **1**−**4**).

Cardiac ligand concentrations are lower than those seen in the plasma, kidney, or liver (Figure 1). However, they again mirror both the plasma and the liver concentrations with the more lipophilic ligands at higher levels. The highest cardiac levels are achieved by the (*S*)-3′,4′-dimethoxy analogue (**5**), 259 nmol/g wet weight at 0.5 h ($p < 0.003$ for **1**−**3** and $p < 0.03$ vs **4**), dropping to 3 nmol/g wet weight at 8 h. The next most effectively concentrated chelator was (*S*)-5′-(CH_3O)-DADFT (**4**). Although its initial 0.5 h level, 208 nmol/g wet weight, was lower than **5**, it surpassed **5** at 1 h and remained higher for 8 h.

Of all the tissues, the pancreas presented with the least amount of ligand accumulation (Figure 1). In this organ (*S*)-5′-(CH_3O)-DADFT (**4**) achieved the highest tissue levels at all time points, although still reaching only 153 nmol/g wet weight at 1 h.

Desazadesmethyldesferrithiocin Analogues. The DADM-DFT analogues in the plasma (Figure 2) are similar to their DADFT counterparts (Figure 1); the more lipophilic systems achieve much higher concentrations and maintain them for a longer period of time. The less lipophilic parent drug (*S*)-4′-(HO)-DADMDFT (**7**) reaches a level of 209 μM at 0.5 h and drops to 5 μM at 2 h. The more lipophilic (*S*)-4′-(CH_3O)-DADMDFT (**8**; plus its metabolite **7**) achieves a concentration of 774 μM at 0.5 h postdrug ($p < 0.001$). At 2 h, the plasma concentration is still greater than 200 μM (Figure 2). A similar scenario is true for (*S*)-5′-(HO)-DADMDFT (**9**) and its methoxy analogue (*S*)-5′-(CH_3O)-DADMDFT (**10**; $p < 0.001$). It is noteworthy that, while the 5′-substituted parent ligand **9** achieves a higher plasma level than its 4′-substituted counterpart **7**, the difference between the 5′-substituted compounds (**9** vs **10**) is not as great as that seen with the 4′-substituted drugs (**7** vs **8**). The (*S*)-3′,4′-(CH_3O)_2-DADMDFT analogue (**11**) also achieves a high initial plasma concentration (695 μM), although it is essentially gone by 4 h.

The renal data for the DADMDFT series (Figure 2) is similar to the DADFT findings (Figure 1). Initially, at 0.5 h, the less lipophilic parent ligands (*S*)-4′-(HO)-DADMDFT (**7**; 667 nmol/g wet weight) and (*S*)-5′-(HO)-DADMDFT (**9**; 629 nmol/g wet weight) are at levels slightly higher than their methoxy counter-

parts **8** and **10**, respectively, though this difference was only significant with **9** vs **10**, $p < 0.05$. However, the parent ligands **7** and **9** diminish far more quickly than the methoxy analogues (Figure 2). There is not nearly as great an initial difference in concentration between the dimethoxy analogue **11** and **7**−**10** as seen in the DADFT series (Figure 1). It is notable that at 0.5 h, (*S*)-4′-(HO)-DADMDFT (**7**) and (*S*)-4′-(CH_3O)-DADMDFT (**8**) both reach over twice the level in kidney tissue as their DADFT counterparts **1** and **2** (Figures 1 and 2).

In the liver (Figure 2), the more lipophilic ligands achieve higher concentrations (**8** > **7** and **10** > **9**). The difference in concentration between the ligands is greater than in the renal tissue. The 4′-(CH_3O) analogue **8** (plus its metabolite **7**) rises to a level of 615 nmol/g wet weight, nearly three times that of the parent (**7**) 0.5 h postdrug ($p < 0.001$). In the case of the 5′-(CH_3O) analogue, the concentration of **10**, 564 nmol/g wet weight, reaches over three times that of the parent **9** ($p < 0.01$). The dimethoxy analogue **11** is greater in concentration than **7**−**10** ($p < 0.001$ for **7**−**9** and $p < 0.02$ vs **10**) but drops off quickly. However, ligand **10** has the longest residence time (Figure 2).

The most notable observation in the DADMDFT series relates to cardiac drug levels (Figure 2). The cardiac tissue presents with the largest differences in concentration between the parent ligands and the methoxylated counterparts (**8** ≫ **7**, $p < 0.002$, and **10** ≫ **9**, $p < 0.002$). It is particularly interesting that (*S*)-5′-(CH_3O)-DADMDFT (**10**) achieves a level of 380 nmol/g wet weight at 0.5 h and remains at 61 nmol/g wet weight even at 4 h. Its parent **9** never rises above 42 nmol/g wet weight Furthermore, ligand **10** also reaches significantly higher concentrations than the (*S*)-3′,4′-dimethoxy chelator **11** (185 nmol/g wet weight, $p < 0.001$).

The scenario is slightly different with the pancreas (Figure 2). The concentration of the 4′-methoxylated ligand **8** (102 nmol/g wet weight) is slightly greater than its hydroxylated counterpart **7** ($p < 0.05$). However, analogue **10** reaches the highest concentration of any of the DADFT or DADMDFT analogues, 198 nmol/g wet weight and is nearly five times greater than its hydroxylated counterpart **9** ($p < 0.02$). Even 4 h postdrug, the tissue concentration is 45 nmol/g wet weight.

Conclusion

There is a pressing need for the continued development of new iron-chelating agents that are either more effective than currently available therapies or can selectively remove iron from organs and tissues especially vulnerable to iron-induced toxicity. Iron-chelating agents that could selectively enter cardiac, pancreatic, or hepatic cells could help immediately reduce toxic iron pools and provide prompt protection against the progression of injury. This is especially true with respect to heart disease, still the leading cause of death in thalassemia major and related forms of transfusional iron overload; the development of such agents could be life-saving.

With early onset of iron overload in which there is no cardiac involvement, the simplest solution is global iron chelation, for example, treatment with DFO or the triazole deferasirox. While

it is true that neither of these ligands achieves notable levels in cardiac tissue, iron contained in all organ systems ultimately equilibrates as the metal is chelated and removed. Thus, cardiac iron is slowly removed but is accessible. However, in a scenario in which iron overload has achieved critical levels in cardiac tissue, ligands that can selectively access this compartment become particularly attractive. The current study is focused on identifying chelators with such organ-specific access. A group of tricoordinate desferrithiocin analogues were assembled (Tables 1 and 2). The ligands belonged to one of two different families, (S)-4,5-dihydro-2-(2-hydroxyphenyl)-4-methyl-4-thia-zolecarboxylic acid (DADFT) or (S)-4,5-dihydro-2-(2-hydroxy-phenyl)-4-thiazolecarboxylic acid (DADMDFT) analogues. The chelators were easily assembled by cyclization of (S)-α-methyl cysteine or (S)-cysteine with the appropriate aromatic nitrile to provide the DADFTs or the DADMDFTs, respectively (Scheme 1). Both the physicochemical properties (log P_{app}) and biological properties—iron-clearing efficiency (ICE) in rodents and primates, toxicity in rodents, and organ distribution in rodents—were measured. The outcome of these measurements was compared and integrated with previous data on related desferrithiocin chelators. The results have led to a number of findings that are critical to future design strategies aimed at the development of organ-specific desferrithiocin ligands belonging to the DADFT or DADMDFT families.

First of all, in rodents, while lipophilicity is a good indicator of how a ligand will perform as an iron chelator, it now seems that the level of the drug achieved in liver tissue (Figure 3) is better. Studies are underway in rodents that will hopefully demonstrate that cardiac ligand tissue levels (Figures 1 and 2) are also a credible indicator for how well a ligand will remove iron from the heart. Although log P_{app} is a good diagnostic tool for ICE in primates, it is only of value when comparing structurally very similar chelators.

Second, there are profound differences in the toxicity between the two families: the DADMDFTs are less toxic than the DADFTs. However, it is possible to impact the toxicity of the DADFTs by reducing their lipophilicity; the less lipophilic the ligand, the less toxic it is (**1**, **3**, and **6** vs **2**, **4**, and **5**, Table 3). The same changes in lipophilicity can have rather profound effects on organ distribution and residence time.

Finally, in the case of the DADFT set, the more lipophilic ligands (**1** vs **2** and **3** vs **4**) achieve and maintain the highest tissue levels, with the exception of the 0.5 h time point in the kidneys. The dimethoxy analogue **5** achieves the highest tissue levels in plasma, kidney, liver, and heart. With the DADMDFT series (**7** vs **8** and **9** vs **10**), the situation is very similar. However, the dimethoxy ligand **11** no longer consistently achieves the highest tissue concentrations. What is most notable, however, is the level of chelator in the heart tissue in this family; the methoxy analogues **8** and **10** achieve and maintain much higher levels in cardiac tissue than their DADFT counterparts **2** and **4**, respectively. The tissue distribution data of (S)-5′-(CH₃O)-DADMDFT (**10**), coupled with its iron-clearing efficiency and toxicity profile, is consistent with the idea that **10** may well serve as an excellent ligand for removing iron from the liver, heart, and pancreas, the most important organs in iron overload.

Experimental Section

C. apella monkeys were obtained from World Wide Primates (Miami, FL). Male Sprague−Dawley rats were procured from Harlan Sprague−Dawley (Indianapolis, IN). Cremophor RH-40 was acquired from BASF (Parsippany, NJ). Ultrapure salts were purchased from Johnson Matthey Electronics (Royston, U.K.). All

hematological and biochemical studies[35] were performed by Antech Diagnostics (Tampa, FL). Atomic absorption (AA) measurements were made on a Perkin-Elmer model 5100 PC (Norwalk, CT). Histopathological analysis was carried out by Florida Vet Path (Bushnell, FL).

Cannulation of Bile Duct in Non-Iron-Overloaded Rats. The cannulation has been described previously.[34,35] Bile samples were collected from male Sprague−Dawley rats (400−450 g) at 3-h intervals for up to 48 h. The urine sample(s) was taken at 24 h intervals. Sample collection and handling are as previously described.[34,35]

Iron Loading of *C. apella* Monkeys. The monkeys (3.5−4 kg) were iron overloaded with intravenous iron dextran as specified in earlier publications to provide about 500 mg of iron per kg of body weight;[44] the serum transferrin iron saturation rose to between 70 and 80%. At least 20 half-lives, 60 d,[45] elapsed before any of the animals were used in experiments evaluating iron-chelating agents.

Primate Fecal and Urine Samples. Fecal and urine samples were collected at 24-h intervals and processed as described previously.[34,35,46] Briefly, the collections began 4 d prior to the administration of the test drug and continued for an additional 5 d after the drug was given. Iron concentrations were determined by flame atomic absorption spectroscopy as presented in other publications.[34,47]

Drug Preparation and Administration. In the iron-clearing experiments, the rats were given a single 150 μmol/kg (**9**) or 300 μmol/kg (**1**−**8**, **10**, **11**) dose of the drugs orally (po). The compounds were administered as (1) a solution in water (**6**); (2) solubilized in 40% Cremophor RH-40/water (**7**, **9**); or (3) the monosodium salt of the compound of interest (prepared by the addition of 1 equiv of NaOH to a suspension of the free acid in distilled water; **1**−**5**, **8**, **10**, **11**).

The drugs were given to the monkeys po at a dose of 150 μmol/kg. The drugs were prepared as for the rats, except that **2** and **8** were solubilized in 40% Cremophor RH-40/water, and compound **9** was administered as its monosodium salt.

Calculation of Iron-Chelator Efficiency. The theoretical iron outputs of the chelators were generated on the basis of a 2:1 complex. The efficiencies in the rats and monkeys were calculated as set forth elsewhere.[37] Data are presented as the mean ± the standard error of the mean; *P*-values were generated via a one-tailed student's *t*-test, in which the inequality of variances was assumed and a *P*-value of <0.05 was considered significant.

Toxicity Evaluation of DADFT and DADMDFT Analogues in Rodents. Male Sprague−Dawley rats (250−300 g) were fasted overnight and were given the DADFT ligands **3**−**5** and the DADMDFT compounds **9**−**11** po by gavage once daily for up to 10 d at a dose of 384 μmol/kg/d. This dose is equivalent to 100 mg/kg/d of the DFT sodium salt. The animals were fed ∼3 h postdrug and had access to food for 5 h before being fasted overnight. Additional animals served as age-matched controls. The animals were monitored at least three times daily, and those found in moribund condition were euthanized. Surviving rodents were sacrificed 1 day after the last dose, and extensive tissues were sent out for histopathological analysis.

Collection of Tissue Distribution Samples from Rodents. Male Sprague−Dawley rats (250−350 g) were given a single sc injection of the monosodium salts of **1**−**5** and **7**−**11** prepared as described above at a dose of 300 μmol/kg. At times 0.5, 1, 2, 4, and 8 h after dosing (*n* = 3 rats per time point), the animals were euthanized by exposure to CO_2 gas. Blood was obtained via cardiac puncture into vacutainers containing sodium citrate. The blood was centrifuged, and the plasma was separated for analysis. The liver, heart, kidneys, and pancreas were then removed from the animals.

Tissue Analytical Methods. The tissue samples were prepared for HPLC analysis by homogenizing them in water at a ratio of 1:2 (w/v). Then, to precipitate proteins, three times the volume of CH₃OH was added, and the mixture was stored at −20 °C for 20 min. This homogenate was centrifuged, and the supernatant was filtered with a 0.2 μm membrane. The filtrate was injected directly onto the column or diluted with mobile phase A (95% buffer [25

mM KH_2PO_4, pH 3.0]/5% CH_3CN), vortexed, and filtered as above prior to injection.

Analytical separation was performed on a Discovery RP Amide C_{16} HPLC system with UV detection at 310 nm, as described previously.[48,49] Mobile phase and chromatographic conditions were as follows: solvent A, 5% CH_3CN/95% buffer; solvent B, 60% CH_3CN/40% buffer.

The concentrations were calculated from the peak area fitted to calibration curves by nonweighted least-squares linear regression with Rainin Dynamax HPLC Method Manager software (Rainin Instrument Co.). The method had a detection limit of 0.5 μM and was reproducible and linear over a range of 1–1000 μM.

Tissue distribution data are presented as the mean; *P*-values were generated via a one-tailed student's *t*-test, in which the inequality of variances was assumed and a *P*-value of <0.05 was considered significant.

Synthetic Methods. Compounds **1**, **2**, and **6**–**8** were synthesized using methods published by this laboratory.[36–39] Amino acid **16** was obtained from Advanced ChemTech, Louisville, KY. Reagents were purchased from Aldrich Chemical Co. (Milwaukee, WI) and Fisher Optima-grade solvents were routinely used. Phosphate buffer was made up to a concentration of 0.1 M at a pH of 6.[50] Reactions were run under a nitrogen atmosphere, and organic extracts were dried with sodium sulfate, which was filtered. Silica gel 40–63 from Silicycle, Inc. (Quebec City, QC, Canada) was used for flash column chromatography. Distilled solvents were employed for reactions involving chelators. Glassware that was presoaked in 3 N HCl for 15 min was used for the isolation of chelators. Melting points are uncorrected. Optical rotations were run at 589 nm (sodium D line) utilizing a Perkin-Elmer 341 polarimeter with *c* as g of compound per 100 mL of DMF (distilled) solution. [^1]H NMR spectra were measured at 400 MHz in DMSO-d_6 (not indicated) or other deuterated solvents, and chemical shifts (δ) are presented in parts per million downfield from tetramethylsilane. Coupling constants (*J*) are in hertz. [^13]C NMR spectra were run at 100 MHz, and chemical shifts (δ) are given in parts per million referenced to the residual solvent resonance in DMSO-d_6 (δ 39.52) or CD$_3$OD (δ 49.00). Elemental analyses were performed by Atlantic Microlabs (Norcross, GA).

(*S*)-2-(2,5-Dihydroxyphenyl)-4,5-dihydro-4-methyl-4-thiazolecarboxylic Acid (3). Compound **15** (12.2 g, 64.8 mmol) was added to a solution of **12** (5.40 g, 40.0 mmol) in degassed CH_3OH (225 mL). Phosphate buffer (150 mL) and $NaHCO_3$ (6.72 g, 80.0 mmol) were added, and the reactants were heated at 70 °C for 40 h with stirring under nitrogen. The reaction mixture was cooled to room temperature, and the solvents were removed by rotary evaporation. The residue was dissolved in saturated $NaHCO_3$ (600 mL) and was washed with EtOAc (3 × 60 mL). The aqueous portion was acidified to pH 2 with cold concentrated HCl. Extraction with EtOAc (4 × 125 mL), solvent removal in vacuo, and recrystallization from EtOAc/hexanes gave 9.83 g (97%) of **3** as brownish yellow crystals, mp 223–224.5 °C: [α]^{24} +28.7° (*c* 1.01); [^1]H NMR δ 1.56 (s, 3 H), 3.36 (d, 1 H, *J* = 11.6), 3.79 (d, 1 H, *J* = 11.6), 6.80 (m, 2 H), 6.88 (m, 1 H), 9.17 (br s, 1 H), 11.72 (br s, 1 H), 13.21 (br s, 1 H); [^13]C NMR δ 24.04, 39.48, 83.01, 114.69, 115.23, 117.59, 121.54, 149.51, 151.29, 170.27, 173.61; HRMS *m/z* calcd for $C_{11}H_{12}NO_4S$, 254.0487 (M + H); found, 254.0479. Anal. ($C_{11}H_{11}NO_4S$) C, H, N.

(*S*)-4,5-Dihydro-2-(2-hydroxy-5-methoxyphenyl)-4-methyl-4-thiazolecarboxylic Acid (4). Sodium bicarbonate (3.88 g, 46.2 mmol) was added to a mixture of **13**[40] (4.607 g, 30.90 mmol) and **15** (6.96 g, 40.6 mmol) in degassed CH_3OH (200 mL) and phosphate buffer (200 mL) to a pH of 6, and the reactants were heated at 60 °C for 2 d with stirring under nitrogen. The reaction mixture was cooled to room temperature, and the volume of the reaction mixture was reduced by rotary evaporation. Cold 0.2 M HCl (280 mL) was added to the residue, which was extracted with EtOAc (150 mL, 2 × 100 mL). The EtOAc layers were washed with saturated NaCl and were concentrated in vacuo to generate 8.21 g (99%) of **4** as yellow solid, mp 126.5–127.5 °C: [α]^{24} +25.9° (*c* 1.06); [^1]H NMR δ 1.59 (s, 3 H), 3.41 (d, 1 H, *J* = 11.6),

3.74 (s, 3 H), 3.83 (d, 1 H, *J* = 12.0), 6.88 (d, 1 H, *J* = 3.2), 6.94 (d, 1 H, *J* = 8.8), 7.09 (dd, 1 H, *J* = 9.2, 3.2), 11.97 (s, 1 H), 13.23 (s, 1 H); [^13]C NMR (CD$_3$OD) δ 24.65, 40.79, 56.30, 84.86, 114.63, 116.91, 118.86, 121.64, 153.57, 154.39, 172.56, 175.80; HRMS *m/z* calcd for $C_{12}H_{14}NO_4S$, 268.0644 (M + H); found, 268.0630. Anal. ($C_{12}H_{13}NO_4S$) C, H, N.

(*S*)-4,5-Dihydro-2-(3,4-dimethoxy-2-hydroxyphenyl)-4-methyl-4-thiazolecarboxylic Acid (5). Sodium bicarbonate (3.50 g, 41.7 mmol) was added to a mixture of **14** (4.855 g, 27.09 mmol) and **15** (6.120 g, 35.66 mmol) in degassed CH_3OH (180 mL) and phosphate buffer (180 mL) to a pH of 6, and the reactants were heated at 66 °C for 2 d 20 h with stirring under nitrogen. The reaction mixture was cooled to room temperature, and the volume of the reaction mixture was reduced by rotary evaporation. Cold 1 M HCl (70 mL) and saturated NaCl (20 mL) were added to the residue, which was extracted with EtOAc (150 mL, 2 × 50 mL). The EtOAc layers were washed with saturated NaCl (70 mL) and were concentrated in vacuo to crude **5**, which was dissolved in DMF (135 mL). Iodoethane (3.0 mL, 38 mmol) and *N,N*-diisopropylethylamine (6.5 mL, 37 mmol) were introduced, and the solution was stirred for 1 d. After solvent removal under high vacuum, the residue was combined with 1:1 0.5 M citric acid/saturated NaCl (200 mL) and was extracted with EtOAc (200 mL, 3 × 50 mL). The combined extracts were washed with 80-mL portions of 0.25 M citric acid, 1% $NaHSO_3$, H_2O, and saturated NaCl, and the solvent was evaporated. Purification by flash column chromatography using 24% EtOAc/pet ether gave the ethyl ester of **5** as a yellow oil: [^1]H NMR (CDCl$_3$) δ 1.30 (t, 3 H, *J* = 7.0), 1.66 (s, 3 H), 3.20 (d, 1 H, *J* = 11.4), 3.86 (d, 1 H, *J* = 11.4), 3.90 and 3.91 (2 s, 6 H), 4.19–4.30 (m, 2 H), 6.48 (d, 1 H, *J* = 9.0), 7.14 (d, 1 H, *J* = 9.0), 12.72 (s, 1 H). The oil was treated with a solution of 50% NaOH (18.64 g, 0.233 mol) and CH_3OH (350 mL) with brief ice bath cooling. After stirring for 1 d at room temperature, solvents were removed by rotary evaporation. Dilute NaCl (210 mL) was added, followed by extraction with Et$_2$O (3 × 60 mL). Cold 2 N HCl (130 mL) was added to the aqueous layer, which was extracted with EtOAc (170 mL, 3 × 80 mL). The EtOAc layers were washed with saturated NaCl (60 mL) and were concentrated in vacuo, furnishing 4.79 g (60%) of **5** as a light green solid: [α]^{24} +45.7° (*c* 1.16); [^1]H NMR δ 1.59 (s, 3 H), 3.37 (d, 1 H, *J* = 11.2), 3.71 (s, 3 H), 3.79 (d, 1 H, *J* = 11.6), 3.84 (s, 3 H), 6.67 (d, 1 H, *J* = 8.8), 7.12 (d, 1 H, *J* = 8.8), 12.72 (s, 1 H), 13.21 (br s, 1 H); [^13]C NMR (CD$_3$OD) δ 24.70, 40.57, 56.53, 60.89, 84.26, 104.43, 112.34, 127.37, 137.46, 154.49, 157.98, 172.63, 175.87; HRMS *m/z* calcd for $C_{13}H_{16}NO_5S$, 298.0749 (M + H); found, 298.0735.

(*S*)-2-(2,5-Dihydroxyphenyl)-4,5-dihydro-4-thiazolecarboxylic Acid (9). Sodium bicarbonate (4.37 g, 52.0 mmol) was added to a mixture of **12** (4.088 g, 30.26 mmol) and **16** (8.19 g, 46.6 mmol) in degassed CH_3OH (220 mL) and phosphate buffer (220 mL) to a pH of 6, and the reactants were heated at 65 °C for 2 d with stirring under nitrogen. The reaction mixture was cooled to room temperature, and the volume of the reaction mixture was reduced by rotary evaporation. Cold 0.5 M HCl (150 mL) was added, followed by extraction with EtOAc (150 mL, 2 × 100 mL). The EtOAc layers were washed with saturated NaCl (80 mL) and were concentrated in vacuo. Recrystallization from aqueous EtOH gave 5.395 g (75%) of **9** as yellow crystals, mp 233–234.5 °C (dec): [α]^{23} −8.5° (*c* 1.18); [^1]H NMR δ 3.62 (dd, 1 H, *J* = 11.4, 7.4), 3.70 (dd, 1 H, *J* = 11, 9.4), 5.46 (dd, 1 H, *J* = 9.4, 7.4), 6.81–6.85 (m, 2 H), 6.89 (dd, 1 H, *J* = 9, 2.6), 9.20 (s, 1 H), 11.74 (s, 1 H), 13.22 (s, 1 H); [^13]C NMR δ 33.45, 76.56, 114.93, 115.29, 117.65, 121.59, 149.53, 151.30, 171.37, 172.31; HRMS *m/z* calcd for $C_{10}H_{10}NO_4S$, 240.0330 (M + H); found, 240.0262. Anal. ($C_{10}H_9NO_4S$) C, H, N.

(*S*)-4,5-Dihydro-2-(2-hydroxy-5-methoxyphenyl)-4-thiazolecarboxylic Acid (10). Sodium bicarbonate (3.83 g, 45.6 mmol) was added to a mixture of **13**[40] (4.600 g, 30.85 mmol) and **16** (7.136 g, 40.64 mmol) in degassed CH_3OH (200 mL) and phosphate buffer (200 mL) to a pH of 6, and the reactants were heated at 60 °C for 3 d 17 h with stirring under nitrogen. The reaction mixture was

cooled to room temperature, and the volume of the reaction mixture was reduced by rotary evaporation. Cold 0.3 M HCl (200 mL) was added, followed by extraction with EtOAc (2 × 150 mL, 3 × 50 mL). The EtOAc layers were washed with saturated NaCl (50 mL) and were concentrated in vacuo. Recrystallization from EtOAc/hexanes afforded 5.999 g (77%) of **10** as a pale green solid, mp 139.5−142 °C: $[\alpha]^{23}$ −7.1° (*c* 1.20); ^{1}H NMR δ 3.64 (dd, 1 H, *J* = 11.2, 7.6), 3.69−3.76 (m, 1 H), 3.74 (s, 3 H), 5.48 (dd, 1 H, *J* = 9.2, 7.6), 6.90 (d, 1 H, *J* = 3), 6.95 (d, 1 H, *J* = 9), 7.10 (dd, 1 H, *J* = 9, 3), 11.97 (s, 1 H), 13.23 (s, 1 H); ^{13}C NMR δ 33.60, 55.67, 76.46, 113.42, 115.36, 117.91, 120.74, 151.68, 152.54, 171.32, 172.35; HRMS *m/z* calcd for $C_{11}H_{12}NO_4S$, 254.0487 (M + H); found, 254.0516. Anal. ($C_{11}H_{11}NO_4S$) C, H, N.

(*S*)-4,5-Dihydro-2-(3,4-dimethoxy-2-hydroxyphenyl)-4-thia-zolecarboxylic Acid (11). Sodium bicarbonate (4.24 g, 50.5 mmol) was added to a mixture of **14** (6.05 g, 33.8 mmol) and **16** (7.95 g, 45.3 mmol) in degassed CH_3OH (225 mL) and phosphate buffer (225 mL) to a pH of 6, and the reactants were heated at 65 °C for 2 d 19 h with stirring under nitrogen. The reaction mixture was cooled to room temperature, and the volume of the reaction mixture was reduced by rotary evaporation. Cold 1 M HCl (67 mL) was added to the chilled mixture, which was extracted with EtOAc (200 mL, 4 × 50 mL) while adding salt. The EtOAc layers were washed with saturated NaCl (50 mL) and were concentrated in vacuo. Recrystallization from EtOAc/hexanes afforded 7.317 g (76%) of **11** as pale yellow crystals, mp 124.5−127.5 °C: $[\alpha]^{24}$ +13.5° (*c* 0.92); ^{1}H NMR δ 3.61 (dd, 1 H, *J* = 11.2, 7.2), 3.66−3.72 (m + s, 4 H), 3.84 (s, 3 H), 5.44 (dd, 1 H, *J* = 9.4, 7.4), 6.68 (d, 1 H, *J* = 8.8), 7.18 (d, 1 H, *J* = 8.8), 12.71 (s, 1 H), 13.19 (br s, 1 H); ^{13}C NMR δ 33.27, 55.95, 59.82, 75.99, 103.80, 110.54, 126.11, 135.90, 152.94, 156.32, 171.43, 172.46; HRMS *m/z* calcd for $C_{12}H_{14}NO_5S$, 284.0593 (M + H); found, 284.0606. Anal. ($C_{12}H_{13}NO_5S$) C, H, N.

2,5-Dihydroxybenzonitrile (12). Boron tribromide (1 M in CH_2Cl_2, 300 mL, 0.3 mol) was added dropwise to **17** (12.24 g, 75.00 mmol) in CH_2Cl_2 (30 mL) with dry ice/acetone cooling. The reaction solution was allowed to warm to room temperature and was stirred for 18 h. After quenching with H_2O (100 mL) with ice-bath cooling, solids were filtered, and the layers of the filtrate were separated. The aqueous phase was diluted with H_2O (200 mL), was adjusted to pH 2 with 1 N HCl, and was extracted with EtOAc (3 × 150 mL). The extracts were concentrated in vacuo, and the residue was recrystallized from EtOAc/hexanes, producing 8.5 g (80%) of **12** as a pale brown solid, mp 167−169 °C (lit[51] 163−165 °C): ^{1}H NMR (CD_3OD) δ 6.78 (d, 1 H, *J* = 8.8), 6.85 (d, 1 H, *J* = 2.8), 6.92 (dd, 1 H, *J* = 3.2, 2.8); ^{13}C NMR (CD_3OD) δ 100.27, 117.82, 118.12, 118.71, 123.48, 151.29, 154.70.

3,4-Dimethoxy-2-hydroxybenzonitrile (14). Compound **19** (21.17 g, 0.1074 mol) and acetic anhydride (96 mL, 1.02 mol) were heated at reflux for 8 h under a Drierite tube. The reaction mixture was concentrated by rotary evaporation and was partitioned between $CHCl_3$ (300 mL) and 8% $NaHCO_3$ (250 mL). After further extraction with $CHCl_3$ (2 × 100 mL), the organic phase was washed with 4% $NaHCO_3$ (100 mL) and saturated NaCl (100 mL), followed by solvent removal in vacuo. The residue was treated with a solution of 50% NaOH (41 mL, 0.78 mol) and CH_3OH (300 mL) with brief ice bath cooling. After stirring for 19 h at room temperature, solvents were removed by rotary evaporation. The residue was treated with 2 N HCl (400 mL) and was extracted with EtOAc (300 mL, 2 × 100 mL). The EtOAc layers were washed with saturated NaCl (100 mL) and were concentrated in vacuo. The crude product was purified by flash chromatography (7% acetone/CH_2Cl_2) and by recrystallization from EtOAc/hexanes to furnish 15.85 g (82%) of **14** as white crystals, mp 153−154.5 °C: ^{1}H NMR δ 3.69 (s, 3 H), 3.86 (s, 3 H), 6.68 (d, 1 H, *J* = 8.8), 7.34 (d, 1 H, *J* = 8.8), 10.44 (s, 1 H); ^{13}C NMR δ 56.19, 60.48, 92.72, 104.86, 117.03, 128.63, 136.30, 153.60, 157.21; HRMS *m/z* calcd for C_9H_{10}-NO_3, 180.0661 (M + H); found, 180.0681. Anal. ($C_9H_9NO_3$) C, H, N.

3,4-Dimethoxy-2-hydroxybenzaldehyde Oxime (19). Hydroxyl-amine hydrochloride (13.34 g, 0.1920 mol) and NaOAc (15.76 g,

0.1921 mol) were added to a warmed solution of **18**[41,42] (23.29 g, 0.1278 mol) in CH_3OH (150 mL). The reaction mixture was heated at reflux for 1 h under a Drierite tube. The reaction mixture was concentrated by rotary evaporation, and the residue was diluted with saturated NaCl (200 mL) and 0.5 M citric acid (100 mL) and was extracted with EtOAc (300 mL, 2 × 100 mL). The EtOAc layers were washed with H_2O (100 mL) and saturated NaCl (100 mL) and were concentrated in vacuo. Recrystallization from EtOAc/hexanes afforded 21.22 g (84%) of **19** as pale yellow crystals, mp 111.5−112 °C: ^{1}H NMR δ 3.69 (s, 3 H), 3.80 (s, 3 H), 6.60 (d, 1 H, *J* = 8.6), 7.17 (d, 1 H, *J* = 9.0), 8.25 (s, 1 H), 9.98 (s, 1 H), 11.18 (s, 1 H); ^{13}C NMR δ 55.78, 59.98, 103.94, 112.62, 123.42, 136.10, 148.28, 150.05, 154.12; HRMS *m/z* calcd for $C_9H_{12}NO_4$, 198.0766 (M + H); found, 198.0759. Anal. ($C_9H_{11}NO_4$) C, H, N.

Supporting Information Available: Elemental analytical data for synthesized compounds. This material is available free of charge via the Internet at http://pubs.acs.org.

References

(1) Raymond, K. N.; Carrano, C. J. Coordination Chemistry and Microbial Iron Transport. *Acc. Chem. Res.* **1979**, *12*, 183−190.

(2) Byers, B. R.; Arceneaux, J. E. Microbial Iron Transport: Iron Acquisition by Pathogenic Microorganisms. *Met. Ions Biol. Syst.* **1998**, *35*, 37−66.

(3) Bergeron, R. J. Iron: A Controlling Nutrient in Proliferative Processes. *Trends Biochem. Sci.* **1986**, *11*, 133−136.

(4) Theil, E. C.; Huynh, B. H. Ferritin Mineralization: Ferroxidation and Beyond. *J. Inorg. Biochem.* **1997**, *67*, 30.

(5) Kalinowski, D. S.; Richardson, D. R. The Evolution of Iron Chelators for the Treatment of Iron Overload Disease and Cancer. *Pharmacol. Rev.* **2005**, *57*, 547−583.

(6) Brittenham, G. M. Disorders of Iron Metabolism: Iron Deficiency and Overload. In *Hematology: Basic Principles and Practice*, 3rd ed.; Hoffman, R., Benz, E. J., Shattil, S. J., Furie, B., Cohen, H. J., et al., Eds.; Churchill Livingstone: New York, 2000; pp 397−428.

(7) Graf, E.; Mahoney, J. R.; Bryant, R. G.; Eaton, J. W. Iron-Catalyzed Hydroxyl Radical Formation. Stringent Requirement for Free Iron Coordination Site. *J. Biol. Chem.* **1984**, *259*, 3620−3624.

(8) Halliwell, B. Free Radicals and Antioxidants: A Personal View. *Nutr. Rev.* **1994**, *52*, 253−265.

(9) Halliwell, B. Iron, Oxidative Damage, and Chelating Agents. In *The Development of Iron Chelators for Clinical Use*; Bergeron, R. J., Brittenham, G. M., Eds.; CRC: Boca Raton, 1994; pp 33−56.

(10) Koppenol, W. Kinetics and Mechanism of the Fenton Reaction: Implications for Iron Toxicity. In *Iron Chelators: New Development Strategies*; Badman, D. G., Bergeron, R. J., Brittenham, G. M., Eds.; Saratoga: Ponte Vedra Beach, FL, 2000; pp. 3−10.

(11) Babbs, C. F. Oxygen Radicals in Ulcerative Colitis. *Free Radical Biol. Med.* **1992**, *13*, 169−181.

(12) Hazen, S. L.; d'Avignon, A.; Anderson, M. M.; Hsu, F. F.; Heinecke, J. W. Human Neutrophils Employ the Myeloperoxidase-Hydrogen Peroxide-Chloride System to Oxidize α-Amino Acids to a Family of Reactive Aldehydes. Mechanistic Studies Identifying Labile Intermediates along the Reaction Pathway. *J. Biol. Chem.* **1998**, *273*, 4997−5005.

(13) Olivieri, N. F.; Brittenham, G. M. Iron-chelating Therapy and the Treatment of Thalassemia. *Blood* **1997**, *89*, 739−761.

(14) Vichinsky, E. P. Current Issues with Blood Transfusions in Sickle Cell Disease. *Semin. Hematol.* **2001**, *38*, 14−22.

(15) Kersten, M. J.; Lange, R.; Smeets, M. E.; Vreugdenhil, G.; Roozendaal, K. J.; Lameijer, W.; Goudsmit, R. Long-Term Treatment of Transfusional Iron Overload with the Oral Iron Chelator Deferi-prone (L1): A Dutch Multicenter Trial. *Ann. Hematol.* **1996**, *73*, 247−252.

(16) Conrad, M. E.; Umbreit, J. N.; Moore, E. G. Iron Absorption and Transport. *Am. J. Med. Sci.* **1999**, *318*, 213−229.

(17) Lieu, P. T.; Heiskala, M.; Peterson, P. A.; Yang, Y. The Roles of Iron in Health and Disease. *Mol. Aspects Med.* **2001**, *22*, 1−87.

(18) Angelucci, E.; Brittenham, G. M.; McLaren, C. E.; Ripalti, M.; Baronciani, D.; Giardini, C.; Galimberti, M.; Polchi, P.; Lucarelli, G. Hepatic Iron Concentration and Total Body Iron Stores in Thalassemia Major. *N. Engl. J. Med.* **2000**, *343*, 327−331.

(19) Bonkovsky, H. L.; Lambrecht, R. W. Iron-Induced Liver Injury. *Clin. Liver Dis.* **2000**, *4*, 409−429, vi-vii.

(20) Pietrangelo, A. Mechanism of Iron Toxicity. *Adv. Exp. Med. Biol.* **2002**, *509*, 19−43.

(21) Cario, H.; Holl, R. W.; Debatin, K. M.; Kohne, E. Insulin Sensitivity and β-Cell Secretion in Thalassaemia Major with Secondary Haemochromatosis: Assessment by Oral Glucose Tolerance Test. *Eur. J. Pediatr.* **2003**, *162*, 139−146.

(22) Wojcik, J. P.; Speechley, M. R.; Kertesz, A. E.; Chakrabarti, S.; Adams, P. C. Natural History of C282Y Homozygotes for Hemochromatosis. *Can. J. Gastroenterol.* **2002**, *16*, 297−302.

(23) Brittenham, G. M.; Griffith, P. M.; Nienhuis, A. W.; McLaren, C. E.; Young, N. S.; Tucker, E. E.; Allen, C. J.; Farrell, D. E.; Harris, J. W. Efficacy of Deferoxamine in Preventing Complications of Iron Overload in Patients with Thalassemia Major. *N. Engl. J. Med.* **1994**, *331*, 567−573.

(24) Zurlo, M. G.; De Stefano, P.; Borgna-Pignatti, C.; Di Palma, A.; Piga, A.; Melevendi, C.; Di Gregorio, F.; Burattini, M. G.; Terzoli, S. Survival and Causes of Death in Thalassaemia Major. *Lancet* **1989**, *2*, 27−30.

(25) Chua, A. C. G.; Olynyk, J. K.; Leedman, P. J.; Trinder, D. Nontransferrin-Bound Iron Uptake by Hepatocytes Is Increased in the *Hfe* Knockout Mouse Model of Hereditary Hemochromatosis. *Blood* **2004**, *104*, 1519−1525.

(26) Oudit, G. Y.; Sun, H.; Trivieri, M. G.; Koch, S. E.; Dawood, F.; Ackerley, C.; Yazdanpanah, M.; Wilson, G. J.; Schwartz, A.; Liu, P. P.; Backx, P. H. L-type Ca^{2+} Channels Provide a Major Pathway for Iron Entry into Cardiomyocytes in Iron-Overload Cardiomyopathy. *Nat. Med.* **2003**, *9*, 1187−1194.

(27) Brittenham, G. M. Iron Chelators and Iron Toxicity. *Alcohol* **2003**, *30*, 151−158.

(28) Davis, B. A.; Porter, J. B. Long-Term Outcome of Continuous 24-Hour Deferoxamine Infusion via Indwelling Intravenous Catheters in High-Risk β-Thalassemia. *Blood* **2000**, *95*, 1229−1236.

(29) Davis, B. A.; Porter, J. B. Results of Long Term Iron Chelation Treatment with Deferoxamine. *Adv. Exp. Med. Biol.* **2002**, *509*, 91−125.

(30) Naegeli, H.-U.; Zähner, H. Metabolites of Microorganisms. Part 193. Ferrithiocin. *Helv. Chim. Acta* **1980**, *63*, 1400−1406.

(31) Hahn, F. E.; McMurry, T. J.; Hugi, A.; Raymond, K. N. Coordination Chemistry of Microbial Iron Transport. 42. Structural and Spectroscopic Characterization of Diastereomeric Cr(III) and Co(III) Complexes of Desferriferrithiocin. *J. Am. Chem. Soc.* **1990**, *112*, 1854−1860.

(32) Anderegg, G.; Räber, M. Metal Complex Formation of a New Siderophore Desferrithiocin and of Three Related Ligands. *J. Chem. Soc., Chem. Commun.* **1990**, 1194−1196.

(33) Bergeron, R. J.; Wiegand, J.; Dionis, J. B.; Egli-Karmakka, M.; Frei, J.; Huxley-Tencer, A.; Peter, H. H. Evaluation of Desferrithiocin and Its Synthetic Analogues as Orally Effective Iron Chelators. *J. Med. Chem.* **1991**, *34*, 2072−2078.

(34) Bergeron, R. J.; Streiff, R. R.; Wiegand, J.; Vinson, J. R. T.; Luchetta, G.; Evans, K. M.; Peter, H.; Jenny, H.-B. A Comparative Evaluation of Iron Clearance Models. *Ann. N. Y. Acad. Sci.* **1990**, *612*, 378−393.

(35) Bergeron, R. J.; Streiff, R. R.; Creary, E. A.; Daniels, R. D., Jr.; King, W.; Luchetta, G.; Wiegand, J.; Moerker, T.; Peter, H. H. A Comparative Study of the Iron-Clearing Properties of Desferrithiocin Analogues with Desferrioxamine B in a *Cebus* Monkey Model. *Blood* **1993**, *81*, 2166−2173.

(36) Bergeron, R. J.; Wiegand, J.; Weimar, W. R.; Vinson, J. R. T.; Bussenius, J.; Yao, G. W.; McManis, J. S. Desazadesmethyldesferrithiocin Analogues as Orally Effective Iron Chelators. *J. Med. Chem.* **1999**, *42*, 95−108.

(37) Bergeron, R. J.; Wiegand, J.; McManis, J. S.; McCosar, B. H.; Weimar, W. R.; Brittenham, G. M.; Smith, R. E. Effects of C-4 Stereochemistry and C-4′ Hydroxylation on the Iron Clearing Efficiency and Toxicity of Desferrithiocin Analogues. *J. Med. Chem.* **1999**, *42*, 2432−2440.

(38) Bergeron, R. J.; Wiegand, J.; McManis, J. S.; Bussenius, J.; Smith, R. E.; Weimar, W. R. Methoxylation of Desazadesferrithiocin Analogues: Enhanced Iron Clearing Efficiency. *J. Med. Chem.* **2003**, *46*, 1470−1477.

(39) Bergeron, R. J.; Wiegand, J.; McManis, J. S.; Vinson, J. R. T.; Yao, H.; Bharti, N.; Rocca, J. R. (*S*)-4,5-Dihydro-2-(2-hydroxy-4-hydroxyphenyl)-4-methyl-4-thiazolecarboxylic Acid Polyethers: A Solution to Nephrotoxicity. *J. Med. Chem.* **2006**, *49*, 2772−2783.

(40) Shinoda, J. The Constitution of Gentisin. *J. Chem. Soc.* **1927**, 1983−1985.

(41) Singh, S. B.; Pettit, G. R. Antineoplastic Agents. 166. Isolation, Structure, and Synthesis of Combretastatin C-1. *J. Org. Chem.* **1989**, *54*, 4105−4114.

(42) Chantimakorn, V.; Nimgirawath, S. Syntheses of the Benzylisoquinoline Alkaloids Isosevanine and Berbithine. *Aust. J. Chem.* **1989**, *42*, 209−213.

(43) Bergeron, R. J.; Wiegand, J.; McManis, J. S.; Weimar, W. R.; Park, J.-H.; Eiler-McManis, E.; Bergeron, J.; Brittenham, G. M. Partition-Variant Desferrithiocin Analogues: Organ Targeting and Increased Iron Clearance. *J. Med. Chem.* **2005**, *48*, 821−831.

(44) Bergeron, R. J.; Streiff, R. R.; Wiegand, J.; Luchetta, G.; Creary, E. A.; Peter, H. H. A Comparison of the Iron-Clearing Properties of 1,2-Dimethyl-3-hydroxypyrid-4-one, 1,2-Diethyl-3-hydroxypyrid-4-one, and Deferoxamine. *Blood* **1992**, *79*, 1882−1890.

(45) Wood, J. K.; Milner, P. F.; Pathak, U. N. The Metabolism of Iron-Dextran Given as a Total-Dose Infusion to Iron Deficient Jamaican Subjects. *Br. J. Haematol.* **1968**, *14*, 119−129.

(46) Bergeron, R. J.; Wiegand, J.; Brittenham, G. M. HBED: A Potential Alternative to Deferoxamine for Iron-Chelating Therapy. *Blood* **1998**, *91*, 1446−1452.

(47) Bergeron, R. J.; Wiegand, J.; Wollenweber, M.; McManis, J. S.; Algee, S. E.; Ratliff-Thompson, K. Synthesis and Biological Evaluation of Naphthyldesferrithiocin Iron Chelators. *J. Med. Chem.* **1996**, *39*, 1575−1581.

(48) Bergeron, R. J.; Wiegand, J.; Weimar, W. R.; McManis, J. S.; Smith, R. E.; Abboud, K. A. Iron Chelation Promoted by Desazadesferrithiocin Analogues: An Enantioselective Barrier. *Chirality* **2003**, *15*, 593−599.

(49) Bergeron, R. J.; Wiegand, J.; Ratliff-Thompson, K.; Weimar, W. R. The Origin of the Differences in (*R*)- and (*S*)-Desmethyldesferrithiocin: Iron-Clearing Properties. *Ann. N. Y. Acad. Sci.* **1998**, *850*, 202−216.

(50) Gomori, G. Preparation of Buffers for Use in Enzyme Studies. *Methods Enzymol.* **1955**, *1*, 138−146.

(51) Römer, A.; Sammet, M. Synthesis of Substituted Phenazines from Benzofurazanoxid and Hydroquinones. *Z. Naturforsch., B: Chem. Sci.* **1983**, *38B*, 866−872.

(52) Bergeron, R. J.; Huang, G.; Weimar, W. R.; Smith, R. E.; Wiegand, J.; McManis, J. S. Desferrithiocin Analogue-Based Hexacoordinate Iron(III) Chelators. *J. Med. Chem.* **2003**, *46*, 16−24.